Journal of Industrial Information Integration 28 (2022) 100366

Contents lists available at ScienceDirect

Journal of Industrial Information Integration

journal homepage: www.sciencedirect.com/journal/journal-of-industrial-information-integration

Design of robot automatic navigation under computer intelligent algorithm and machine vision

Pengcheng Wei [a], Xianping Yu [b], Zhenpeng Di [c,*], Xiaojun Dai [d], Bo Wang [d], Yushan Zeng [d]

[a] School of Mathematics and Information Engineering, Chongqing University of Education, Chongqing 400065, China
[b] School of Arts and communication, Beijing Normal University, Beijing , Beijing, 100875 China
[c] School of Management Science and Engineering, Guangxi University of Finance and Economics, Nanning, Guangxi, 530003 China
[d] School of Automation, Chongqing University of Posts And Telecommunications, Chongqing 400065, China

A R T I C L E I N F O

Keywords:
Computer intelligence algorithm
Machine vision
Robot
Automatic navigation
Ant colony algorithm

A B S T R A C T

This work aims to explore the robot automatic navigation model under computer intelligent algorithms and machine vision, so that mobile robots can better serve all walks of life. In view of the current situation of high cost and poor work flexibility of intelligent robots, this work innovatively researches and improves the image processing algorithm and control algorithm. In the navigation line edge detection stage, aiming at the low efficiency of the traditional ant colony algorithm, the Canny algorithm is combined to improve it, and a Canny-based ant colony algorithm is proposed to detect the trajectory edge. In addition, the Single Shot MultiBox Detector (SSD) algorithm is adopted to detect obstacles in the navigation trajectory of the robot. The performance is analyzed through simulation. The results show that the navigation accuracy of the Canny-based ant colony algorithm proposed in this work is basically stable at 89.62%, and its running time is the shortest. Further analysis of the proposed SSD neural network through comparison with other neural networks suggests that its feature recognition accuracy reaches 92.90%. The accuracy is at least 3.74% higher versus other neural network algorithms, the running time is stable at about 37.99 s, and the packet loss rate is close to 0. Therefore, the constructed mobile robot automatic navigation model can achieve high recognition accuracy under the premise of ensuring error. Moreover, the data transmission effect is ideal. It can provide experimental basis for the later promotion and adoption of mobile robots in various fields.

1. Introduction

With the rapid progression of science today, all walks of life are developing towards intelligence. As a new product of the progression of science, robots have many functions, such as environmental detection, planning and decision-making, and automatic driving, which promote the rapid progression of social economy. For example, in the medical field, robots assist doctors to complete some complex and delicate operations, which can reduce the error rate and reduce the work burden for doctors. In the construction industry, robots speed up production, save labor costs, and reduce the risk factor of the industry. In the field of logistics, robots replace human to complete the transportation of goods, improving efficiency and saving labor. In the field of household management, robots can recognize the home environment independently, complete the cleaning task, and free people's hands at the same time [1, 2]. Therefore, the adoption of robot mobile model with artificial intelligence (AI) in practical work has become the focus of all walks of life.

As one of the service robots, domestic service and lawn mowing robots can autonomously clean up the ground garbage and mow the lawn by successfully avoiding static or dynamic obstacles in the working environment. Based on the progression of mobile robot, this kind of robot integrates positioning, multi-sensor information fusion, path planning, and other technologies into one. Even when the working environment is relatively complex and the needs are relatively special, they can complete the work [3]. Therefore, path planning for mobile robots is the focus of current scholars in related fields. In addition, the mobile robot must meet the requirements of low repetition rate and high coverage rate when working in the complex and changeable environment.

To traverse the whole environment through the optimal collision free path, it is necessary to study the path planning algorithm of the whole

* Corresponding author.
E-mail address: 2018110034@gxufe.edu.cn (Z. Di).

https://doi.org/10.1016/j.jii.2022.100366

Available online 24 May 2022

area coverage. Whole-area coverage path planning means that the robot can find a suitable obstacle free walking path in the working environment. It can not only cover the whole working area, but also avoid repeating roads as far as possible, so it is essential to identify objects such as obstacles [4,5].

As one of the AI algorithms, machine vision can monitor and distinguish the obstacles in the robot's moving path during its moving process. Through machine vision products, such as image uptake devices, the machine vision model converts the obstacles in the moving path into image information, which is transmitted to a special image operation platform. Then, the body image of the absorbed object is obtained, which is changed into digital data according to the pixel layout, color, and brightness [6]. The image model carries on different arithmetic to this kind of signal to obtain the feature of the target and then controls the scene according to the conclusion of discrimination. As a complex subject integrating multiple courses, deep learning is mainly utilized to imitate or learn human learning and working methods, so as to make AI more reliable and perfect [7]. This algorithm has a strong fault-tolerant level and can learn and train with the help of internal structure. It has a good processing ability for complicated noise data and can accept some defects in samples. To extract the complex road environment information in the robot's moving path, deep learning is utilized to analyze and process images to obtain a lot of environmental information, such as distance, light intensity, and obstacle information, which greatly reduces the production cost [8,9]. Therefore, it is of great significance to apply the image processing of computer vision to the actual work of lawn mowing robot.

To sum up, under the trend of rapid development of science and technology, it is of great practical significance for social development to widely apply the precise automatic navigation and path planning system of mobile robots to all walks of life. The innovation of this work lies in the following points. In view of the current situation of high cost and poor work flexibility of intelligent robots, its image processing algorithm and control algorithm are analyzed and improved. In the navigation line edge detection stage, the Canny algorithm is introduced for improvement and a Canny-based ant colony algorithm is proposed to detect trajectory edges in view of the low efficiency of traditional ant colony algorithm. The SSD algorithm is adopted to detect obstacles in the navigation trajectory of the robot. Finally, simulation is carried out to analyze its performance, which provides experimental basis for the later application of mobile robots in various industries.

2. Related work

2.1. Current situation of mobile robots

With the rapid progression of AI, the adoption field of intelligent mobile robot is more and more extensive. Many researchers studied its path planning, and a variety of different algorithms were utilized to plan its path. Bayat et al. (2018) proposed a path planning method under optimization of the theory of charged particle potential field by studying the path planning problem of mobile robots with scattered obstacles in the visually known environment. The optimal path was obtained from cost function optimization by achieving a trade-off between traversing the shortest path and avoiding conflicts at the same time. It was found that this method was feasible in practice and can be applied to static and dynamic environments to plan a feasible, fast, non-oscillatory, and non-collision path planning [10]. Hosseininejad and Dadkhah (2019) proposed a new method under cuckoo optimization algorithm for path planning of mobile robots in a dynamic environment and optimized its feature vectors to realize that mobile robots are not disturbed by obstacles in the process of moving. It was found that under different environmental conditions, this algorithm had good performance in finding short, safe, smooth, and collision free paths [11]. In works of Wu et al. (2020), a real-time dynamic path planning method for mobile robots was proposed to avoid both static and dynamic obstacles under the hybrid of beetle antennae search (BAS) algorithm and the artificial potential field (APF). It was found that the robot's moving path became closer to the available path in the real environment by setting the safety range for this model, which proved the effectiveness and superiority of this algorithm [12]. Wang et al. (2021) utilized neural networks for path planning of robots in dynamic environments and proposed a new method for neural networks to provide training samples. The training samples of the neural network were constructed by recognizing the coordinates of the target and the obstacle and the motion direction of the robot corresponding to the position relationship. The precise motion direction obtained by the fuzzy artificial potential field algorithm enabled the neural network to have good path optimization capability [13].

2.2. Current situation and trend of machine vision

In industrial visual perception, image processing methods are indispensable, and many scholars conducted research on it. Xin et al. (2018) proposed the improved deep convolutional neural networks (CNN), which expands the width of CNN by adding parallel coil layers. This model helps to extract image features and improve network performance. In the coiling layer, the batch normalization method is adopted to preprocess the feature images to speed up the network training speed. Experimental results showed that the model can learn the image features of cervical cancer cells more accurately and effectively reduce the classification error rate [14]. He et al. (2018) utilized CNN to classify hyperspectral images (HSIS). A new manual feature extraction method under multiscale covariance maps (MCMs) was proposed. The effect of this method was obvious, and the classification accuracy was significantly improved [15]. Sergiyenko and Tyrsa (2020) proposed a 3D optical sensor data transmission algorithm under the principle of dynamic triangulation. Aiming at the improvement of the navigation of the electric wheel mobile robot group in unknown clutter terrain, two different simulation methods were proposed to optimize the fused database and achieve better path planning. The combination of optical laser scanning sensor and intelligent data management made the dead reckoning of robotic group (RG) more effective [16]. Papadopoulos et al. (2021) proposed a new multi-agent learning from demonstration (LfD) robot learning cognitive architecture, which aimed to realize the reliable deployment of open, scalable, and extensible robotic models in large-scale and complex environments, and also illustrated the applicability of the framework [17].

To sum up, through the analysis of the research of the above scholars, it is found that although there are many researches related to robots, there are not many researches on the automatic navigation of their movement trajectory. In this work, an ant colony algorithm under Canny is proposed to detect the edge of the trajectory, and the neural network algorithm is employed to detect the obstacles.

3. Automatic navigation model of mobile robot under machine vision and intelligent algorithm

3.1. Requirements and overall design of mobile robots

Intelligent technology is gradually widely utilized in all walks of life today, and the intellectualization and automation of factories has become its progression direction. The electromagnetic orbit, laser, radar, and other devices involved in obstacle avoidance navigation of intelligent mobile model currently adopted in industry usually have the disadvantages of high cost and poor working flexibility [18,19]. Therefore, it is of great significance to design intelligent mobile model under machine vision after the key road image processing algorithm and obstacle avoidance navigation control algorithm are improved and the effectiveness of the improved algorithm is verified by simulating the production environment in laboratory.

Generally, mobile robots have to collect road image information and

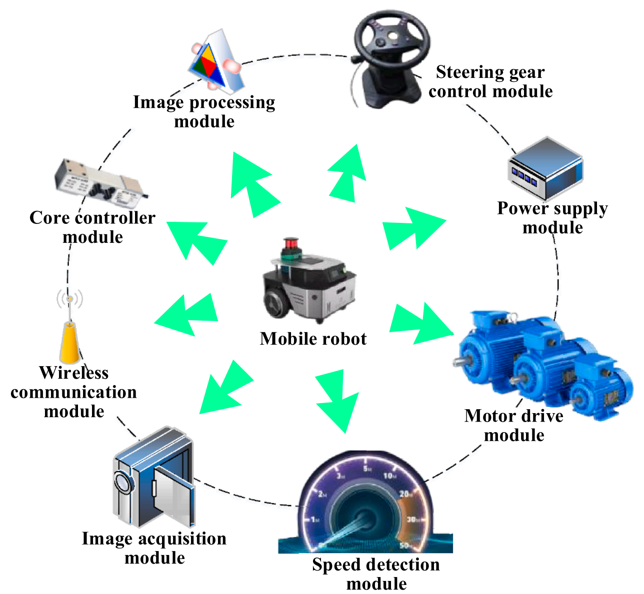

Fig. 1. Modules included in the mobile robot.

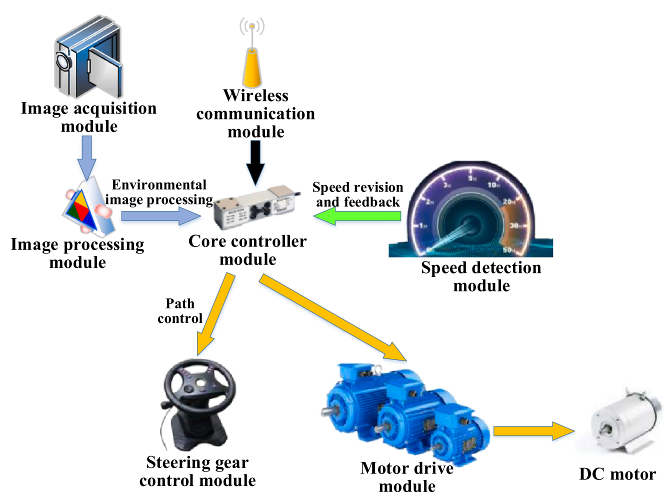

Fig. 2. System hardware module structure framework of mobile robot.

extract road parameter information through the vision sensor part. Then, the motor and steering gear are controlled by a control algorithm to make the model follow the paved navigation line. For some unpredictable obstacles that may exist on the road, machine vision processing algorithm is employed to detect the position, size, shape, and other information of obstacles in the road image, thereby controlling the steering gear to realize the model angle deflection and avoiding obstacles. In this research, the modules included in the mobile robot are shown in Fig. 1.

In the hardware module design for mobile robots in this research, the main functions of the core control module are receiving sensor data, running control algorithms, driving motors and steering gears, and communicating with other digital components. The image processing module is mainly utilized by mobile robots to process road images and surrounding environment information, which also extracts parameter information required for obstacle avoidance navigation. The steering gear control module adjusts the angle of the car body to be executed according to the current path information and motion state of the car body, which then realizes the precise angle adjustment of the model through the steering gear control signal. The power supply module,

Fig. 3. Running process of mobile robot automatic navigation model under machine vision.

through the design of various voltage conversion circuits, enables the power battery to provide a reliable power supply voltage for the normal operation of each module. The motor drive module provides a reliable drive circuit for the motor to realize the model running at a predetermined speed. The speed detection module provides real-time and accurate speed feedback for the control of the motor and ensures stable and smooth vehicle speed by correcting the speed error accurately and quickly. The image acquisition module uses visual sensors to collect road images and surrounding environment information and transmits the information to the image processing module for processing. The wireless communication module transmits the data of the model motion state to the personal computer (PC) control terminal [20] to complete the data transmission between the model and the PC control terminal. The concrete frame structure among the overall hardware of this model is shown as in Fig. 2.

The software design of the mobile robot includes using the image acquisition module to perform image preprocessing operations on the collected road image information, then detecting the edge of the navigation line, and finally extracting the parameter information of the road navigation line. The collected road images are detected to determine whether there are obstacles on the road. If there are obstacles, the obstacles should be detected in real time, and the positional relationship between the obstacles and the vertical center line of the image should be calculated. Algorithmic processing is performed on road parameter information, and motor and steering gear are controlled for visual obstacle avoidance navigation. Fig. 3 shows the running process of the mobile robot's automatic navigation model under machine vision.

As shown in Fig. 3, in the automatic navigation model of the mobile robot, the image processing algorithm and control algorithm are first studied and improved. In the edge detection phase of the navigation line, the traditional ant colony algorithm is combined with the Canny algorithm to improve it against the shortcomings of the low efficiency of the traditional ant colony algorithm. In the obstacle detection process, aiming at the shortcomings of the existing binocular vision algorithm

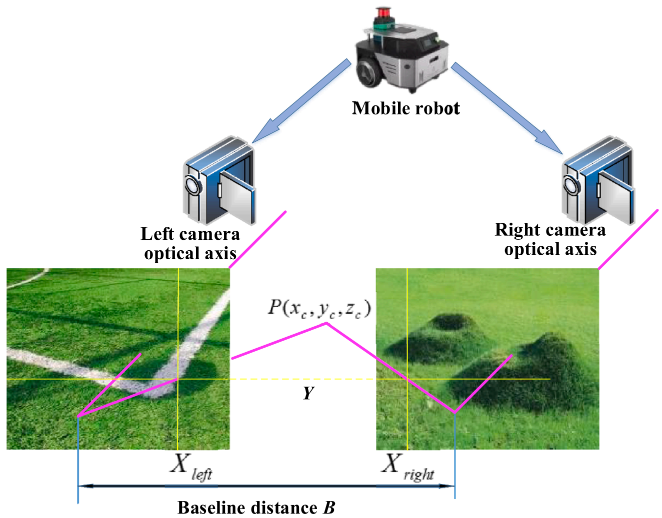

Fig. 4. Binocular vision inspection imaging of mobile robot.

that it is difficult to calibrate and the amount of calculation is large, an integral projection and area growth algorithm are proposed to detect obstacles. After the first frame of obstacle detection image is obtained, the machine learning algorithm is employed for real-time positioning, which improves the detection efficiency and realizes the model's fast and accurate obstacle avoidance navigation.

3.2. Image information detection algorithm for mobile robot automatic navigation

It is very important to select the appropriate navigation in the design of the automatic navigation performance of the intelligent mobile robot. There are many common navigation technologies, such as electromagnetic navigation, laser navigation, and visual navigation. Visual navigation uses visual sensors to perceive environmental information and is more accurate than other sensors [21]. The vision sensor receives the measurement signal passively but does not emit energy by itself, so that it will not affect each other. Moreover, the visual navigation method has high technical requirements. After the road image information is collected, the image is processed, and the navigation line information is extracted to control the motor and the steering gear to complete the model navigation. In the design of mobile robot navigation model, detecting and avoiding obstacles in the path is the key to it. Visual obstacle avoidance refers to using the model to configure the camera to collect road images and using related technologies, such as feature recognition, road extraction, and distance estimation, to process road images. Then, the road navigation line and obstacle information are obtained to guide the mobile robot to avoid obstacles in the model. The key to the problem of visual obstacle avoidance is the detection of obstacles, which usually include monocular vision obstacle detection algorithms and binocular vision detection algorithms [22, 23].

Monocular vision detection uses a single camera to collect the surrounding road conditions and process the acquired environmental data to identify targets. This method can cause the visual change of the captured image due to the change between the relative position of the photographer and the target. Monocular vision detects the relative position information between the target and the photographer under the magnitude of this change. It is assumed that point C is a camera and point P is a real object in space, the imaging point of the target in the image is a point P'. The distance between the camera and the ground is h, the shortest distance from the vertical viewing angle to the ground is y_b, and the longest distance is $y_1 + y_b$. The angle between the projection of the camera's vertical angle of view on the ground and the horizontal ground x and y axis is α, β. The angle between the mapping of the camera's horizontal angle of view on the ground and the y-axis of the ground plane is θ. At this time, according to the monocular pinhole projection model, the following equation is obtained.

$$\alpha = \arctan^{-1}\left(\frac{h}{y_b}\right) \tag{1}$$

$$\beta = \arctan^{-1}\left(\frac{h}{y_1 + y_b}\right) \tag{2}$$

$$\theta = \arctan^{-1}\left(\frac{x_1}{y_1 + y_b}\right) \tag{3}$$

Among them, $h, y_1 + y_b, x_1$ are obtained by measurement, and S_x and S_y are the number of rows and columns of the captured image, respectively. Then, the following equations are obtained.

$$y = h\tan\left((90 - \alpha) + \left(1 + \frac{v}{S_y}\right) \times (\alpha - \beta)\right) \tag{4}$$

$$x = y\tan\left(\left(1 - \frac{v}{S_x}\right) \times \theta\right) \tag{5}$$

$$L = \sqrt{x^2 + y^2} \tag{6}$$

Among them, y is the ordinate of the point $P(x,y)$ in the camera coordinate system xoy, that is, the distance between the target and the device in the vertical direction. x is the abscissa of the point $P(x,y)$ force in the camera coordinate system xoy, that is, the distance between the object and the mobile device in the horizontal direction, and L is the actual distance between the object and the camera.

Binocular parallax uses two cameras at different positions to obtain information about the surrounding environment and then completes the visual image detection task through different algorithms. It mainly includes feature extraction, target matching, geometric modeling, and 3D reconstruction. The model uses dual cameras to observe the scene of the 3D world. Its visual processing method is more similar to that of the human visual model, and the obtained image has a clear sense of depth. The imaging of binocular parallax is shown in Fig. 4.

From Fig. 4, in the binocular imaging model of the mobile robot, the parallax of the two images is as follows.

$$Disparity = X_{left} - X_{right} \tag{7}$$

The 3D coordinates of the midpoint $P(x_c, y_c, z_c)$ of binocular imaging is expressed as the following equation.

$$\begin{cases} x_c = f\dfrac{BX_{left}}{Disparity} \\ y_c = f\dfrac{BY}{Disparity} \\ z_c = \dfrac{BY}{Disparity} \end{cases} \quad (8)$$

Through the above analysis of binocular parallax, it is found that when binocular parallax is adopted to calibrate two cameras, there are problems with calibration difficulties, complex technical processing, and low efficiency. In addition, it is difficult to meet the high real-time requirements of the model. Therefore, an integral projection and area growth algorithm suitable for obstacle detection is proposed for the automatic navigation path of mobile robots [24]. The position of the obstacle in the first frame of image is detected, and then the machine learning algorithm is employed to locate in real time, thereby improving the efficiency and accuracy of obstacle detection.

In the integral projection coarse positioning algorithm, $I(x,y)$ is denoted as the gray value of the pixel at the point (x,y). In the image area, if the gray value of the row or column in the image suddenly changes drastically, this amplitude change will affect the effect of integral projection. Therefore, the integral projection value is utilized to analyze the image and extract features. The vertical integral projection function and the horizontal integral projection function are as follows.

$$V(x) = \sum_{y=1}^{H} f(x,y), y = 1,2,\cdots,H \quad (9)$$

$$L(y) = \sum_{y=1}^{W} f(x,y), x = 1,2,\cdots,W \quad (10)$$

To reduce the search area, the integral projection is adopted to locate the obstacles. Through horizontal integral projection and vertical integral projection of the obstacle image, the calculated pixel curve has a gray maximum or minimum value. Then, the midpoint of the coarse positioning position of the obstacle obtained by integral projection is taken as the seed point, and the region growth is adopted to locate the obstacle fine.

3.3. Automatic navigation model of mobile robot under machine vision

The intelligent mobile robot collects road images through visual sensors, and performs road image preprocessing first, including grayscale, filter processing, and camera calibration. The edge information is extracted by the navigation line edge detection algorithm, and then the navigation line information is extracted, obstacle detection is performed, and finally the steering gear is controlled to perform obstacle avoidance navigation.

After collecting the path information, the mobile robot performs preprocessing operations on the information images in the path, which mainly include grayscale, filter processing, and camera calibration. Generally, gray-scale processing of an image can greatly reduce the amount of calculation and save processing time without affecting most of the texture characteristics of the object. Converting a color image to a grayscale image means mapping from a high-dimensional space to a low-dimensional space. It is supposed that f represents any vector in red-green-blue (RGB) [25] high-dimensional space, which is illustrated as follows.

$$f(x,y) = \begin{bmatrix} f_R \\ f_G \\ f_B \end{bmatrix} = \begin{bmatrix} R \\ G \\ B \end{bmatrix} \quad (11)$$

A color image $f(x,y)$ is composed of a mixture of three RGB channels. The mapping relationship between color components and coordinates is expressed as the following equation.

$$f(x,y) = \begin{bmatrix} f_R(x,y) \\ f_G(x,y) \\ f_B(x,y) \end{bmatrix} = \begin{bmatrix} R(x,y) \\ G(x,y) \\ B(x,y) \end{bmatrix} \quad (12)$$

In the process of gray scale conversion, the commonly utilized methods include maximum value method, weighted average method, and component method. The maximum value method selects the value with the largest weight among the three values of RGB as the gray value of the point.

$$g(x,y) = \max(f_I(x,y)), I = R,G,B \quad (13)$$

The weighted average method refers to multiplying the three component values of RGB and the corresponding weight, and the sum is taken as the gray value. In this method, because the human eye is more sensitive to green, the green part tends to be larger. There is a famous psychological equation: Gray=R*0.299+G*0.587+B*0.114 [26]. The equation of this method is as follows.

$$g(x,y) = \frac{1}{i+j+k}(if_R(x,y) + jf_G(x,y) + kf_B(x,y)) \quad (14)$$

The component-taking method uses one of the three RGB components of a pixel as the gray value of the pixel to obtain a grayscale image. This method is relatively simple and saves resources at the same time.

$$g(x,y) = f_I(x,y), I = R,G,B \quad (15)$$

Through the analysis of the above three methods, the maximum method is finally selected to process the image of the robot moving path in gray. In the subsequent filtering process, the median filtering process is selected, and the value of the pixel is replaced by the median gray value of the neighboring pixels of the pixel.

$$f'(x,y) = \underset{(s,t)\in s_{x,y}}{median}\{g(s,t)\} \quad (16)$$

$g(s,t)$ refers to the gray value corresponding to the pixel at the center of the original image, $f'(x,y)$ is the output after the filter, $s_{x,y}$ refers to the coordinate set in the rectangular area with the center point (x,y) in and the range of $m \times n$. Further preprocessing of the camera calibration is implemented. During the camera calibration of the smart mobile model, although the coordinates of the points in the real physical scene in the camera frame of axes can't be obtained, the coordinates of the points in the specified earth map coordinate can be obtained, as shown in the following equation.

$$\widetilde{q} = sMW\widetilde{Q} \quad (17)$$

In Eq. (17), $\widetilde{q} = (x,y,1)$ and $M = \begin{bmatrix} f_x & 0 & c_x \\ 0 & f_y & c_y \\ 0 & 0 & 1 \end{bmatrix}$. It is set that $Z = 1$, so that $\widetilde{Q} = (X \quad Y \quad 1)$, s can be any scale ratio, and $W = (r_1 \quad r_2 \quad t)$. It is supposed that $H = (h_1 \quad h_2 \quad h_3) = sMW$. Two constraints are obtained as follows from the orthogonality of r_1 and b r_2.

$$h_1^T M^{-T} M^{-1} h_2 = 0 \quad (18)$$

$$h_1^T M^{-T} M^{-1} h_1 = h_2^T M^{-T} M^{-1} h_2 \quad (19)$$

It is set that (x,y) is the coordinates in the image frame of axes without considering the distortion, $(\widetilde{x},\widetilde{y})$ is the real coordinate in the image frame of axes after the distortion, and (x,y) and $(\widetilde{x},\widetilde{y})$ are all normalized, then the corresponding relationship between the two satisfies the following equation.

$$\widetilde{x} = x + \left(k_1\left(x^2+y^2\right) + k_2\left(x^2+y^2\right)^2\right) \quad (20)$$

$$\widetilde{y} = y + \left(k_1\left(x^2+y^2\right) + k_2\left(x^2+y^2\right)^2\right) \quad (21)$$

Among them, k_1 and k_2 are the radial distortion coefficients. By

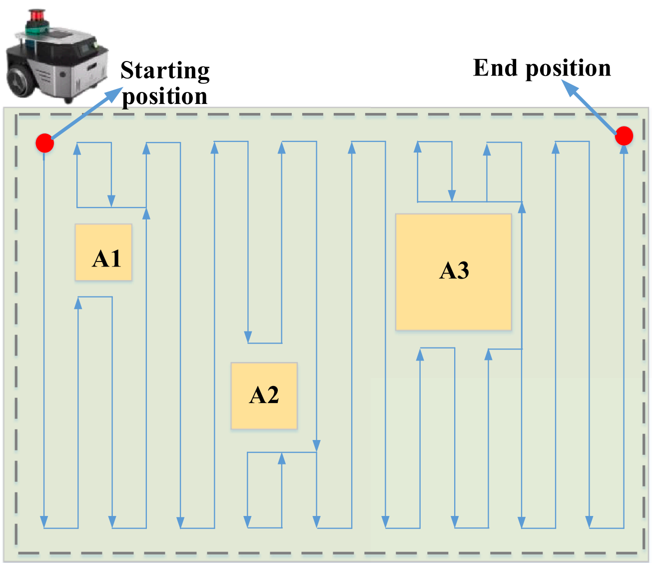

Fig. 5. Schematic diagram of automatic navigation of mobile robot.

point of the prediction box
$w \leftarrow$ The width of the prediction box
$Th = a \times thH + b \times thL$
$a, b \leftarrow$ constant
$h \leftarrow$ The height of the prediction box
Determine the positive and negative samples in the sample set
The objective loss function L is defined as the confidence error L_{conf} and the position error L_{loc}, as shown in equation (24)
The target loss function is utilized to make regression analysis of coordinate migration of prediction frame
CNN back propagation network $\leftarrow$ Adjust the weight of each layer
Elimination of repeated prediction frames by non-maximum suppression algorithm
end Get the result of target detection

Fig. 6. The specific process of the SSD algorithm to detect obstacles.

correcting the distortion of the camera image frame of axes, the actual position of the road surface is accurately described finally.

In this work, when the robot faces an environment with obstacles, its path is automatically navigated as shown in Fig. 5.

As shown in Fig. 5, the lawn mobile robot constructed in this work starts to move according to the Canny-based ant colony algorithm. The first goal is to detect the edges of the trajectory. When an edge is detected, a work path shown in Fig. 5 was constructed (some obstacles have been detected and considered in the work path, some of them are not). Obstacle detection is also active in the first stage to avoid obstacles. Obstacles (A1/A2/A3) are detected using SSD algorithm. Now, the robot starts to move according to the planned path and detects obstacles in real time. This means that the working path will adapt to detected obstacles in real time. Finally, the optimized path is obtained. However, when the mobile robot passes through the same area, it will extract the navigation line information, understand its location, and directly retrieve the edge information detected in the previous stage, thereby avoiding repeated edge detection and reducing the efficiency. The application of related algorithms in obstacle detection and edge detection involved in the path planning process is as follows.

The obstacle detection algorithm uses integral projection and area growth algorithm to detect subjects and then uses deep learning algorithm to locate the obstacle in real time. In the obstacle avoidance navigation research of robots, a combination of Faster RCNN (Regions with CNN features) and YOLO (You Only Look Once: Unified, Real-Time Object Detection) is proposed to fabricate an SSD detection algorithm. The specific process of obstacle detection using SSD algorithm is shown in Fig. 6.

In the training process using the SSD algorithm, the target loss function L is defined as the weighted sum of the confidence error L_{conf} and the position error L_{loc}, and the equation is as follows.

$$L(x, c, l, g) = \frac{1}{N}\left(L_{conf}(x, c) + \alpha L_{loc}(x, l, g)\right) \tag{22}$$

Among them, c refers to the confidence of the target detection category, l refers to the prediction frame parameter, g refers to the real frame parameter, and N refers to the number of matches to the real frame. α is utilized to adjust the ratio between the two types of losses, and the default value is 1. For the confidence error L_{conf}, the softmax loss is utilized for calculation, and the calculation equation is as follows.

$$L_{conf}(x, c) = -\sum_{i \in Pos}^{N} x_{ij}^{p} \log\left(\widehat{c}_j^{p}\right) - \sum_{i \in Neg}^{N} \log\left(\widehat{c}_i^{0}\right) \tag{23}$$

Among them, it is supposed that the i th prediction box has a matching relationship with the j-th real box and when the matching category is p, the value of x_{ij}^{p} is 1, otherwise the value is 0. The calculation equation for confidence $\widehat{c}_j^{p}$ is as follows.

$$L_{loc}(x, l, g) = \sum_{i \in Pos}^{N} \sum_{m} x_{ij}^{k} smooth_{L1}\left(l_i^m - \widehat{g}_j^m\right) \tag{24}$$

The calculation equation of $smooth_{L1}(x)$ in Eq. (24) is shown in Eq. (25).

$$smooth_{L1}(x) = \begin{cases} 0.5x^2 & if |x| < 1 \\ |x| - 0.5 & otherwise \end{cases} \tag{25}$$

The process of training the classifier is described by the following mathematical equation.

$$\min \sum_{i=1}^{m} L(y_i, f(x_i)) + \lambda \| \omega \|^2 \tag{26}$$

The optimal one that minimizes the cost function is found, which is expressed as the following equation.

$$\omega = \sum_{i} a_i \phi(X_i) \tag{27}$$

a_i is the coefficient of the training sample, while $\phi(X_i)$ is a function that maps the training sample x to the high-dimensional feature space. The correlation between any two samples x and x^* in the high-dimensional feature space is $\phi^T(x)\phi(x*) = \mathrm{K}(x, x*)$, where K is a Gaussian function. Therefore, the following equation is obtained.

$$a = (K + \lambda I)^{-1} y \tag{28}$$

K is a kernel matrix constructed from training sample $P^i x, i = 0, 1, \cdots, n-1$, $a = [a_1, a_2, \cdots, a_n]$, and Fourier transform of Eq. (28) is given as the following equation.

$$f(a) = \widehat{a} = \frac{f(y)}{f(k^{xx}) + \lambda} \tag{29}$$

$\widehat{a}$ is discrete Fourier transform of a, and k^{xx} is the first row vector of the kernel matrix K. The process of training the classifier is transformed from searching for the optimal ω to searching for the best.

Furthermore, edge detection is performed on the navigation line of the mobile robot. The ant colony algorithm is employed for research.

Start
Input: Edge heuristic information η, pheromone τ
Output: Navigation line edge
Initialize the number of ants m, the number of cycles n_c, n_c=0
The final threshold Th is obtained by linear combination of high threshold thH and low threshold thL
$Th = a \times thH + b \times thL$
$a, b \leftarrow$ constant
$\eta(i,j) = -1$ //The point is not an edge point
$\eta(i,j) = [0,1]$ //This point is an edge point
Ant's forward direction probability $P_i = \frac{\tau_i^\alpha(t)\eta_i^\beta(t)}{\sum_{i\in S}\tau_i^\alpha(t)\eta_i^\beta(t)}$
$\alpha \leftarrow 0.6, \beta \leftarrow 0.2$
Each ant is limited to walk *rate* steps
$rate = Width \times Height \times dis\_rate$
$dis\_rate \leftarrow (0,1]$
At t +1, the pheromone of pixel i is updated to $\tau_i(t+1)$
$\tau_i(t+1) = (1-\rho) \times \tau_i(t) + \Delta\tau$
$\rho \leftarrow 0.1$
end $Nc = Nc + 1$
Until The number of cycles reaches Nc

Fig. 7. Canny-based ant colony algorithm process.

When the traditional ant colony algorithm detects the edge of the image, since the ants are randomly placed in any position of the image during the initial search, it produces a lot of useless calculations and repetitive actions. It finally leads to a large amount of calculation, low efficiency, and easy to fall into a local optimum, which reduces the efficiency of the algorithm.

In this research, the Canny operator is incorporated, and an ant colony algorithm under Canny is constructed to optimize the path. The edge information is extracted according to the basic principle of Canny operator. After the maximum value of Canny's gradient amplitude is suppressed, the double threshold method is not utilized to extract the edge, but the prior knowledge of the edge point is obtained by linear combination of high and low thresholds. Then, an edge tracking model under the ant colony algorithm is established, and ants are assigned to each pixel extracted by Canny. The ants that terminated abnormally in the previous cycle are also randomly assigned initial positions on the pixels extracted by Canny, which can reduce the distribution of ants in non-edge areas. As for the ants that do not walk on the edge points, the walking is stopped immediately, which can improve the efficiency of the ant colony algorithm. The flow of the ant colony algorithm under Canny is shown in Fig. 7.

The Canny algorithm is combined to improve the traditional ant colony algorithm. The Canny algorithm is employed to detect possible edge points and noise points, and heuristic information is established. The edge tracking model of ant colony algorithm is essentially to extract edge points and eliminate noise points from the heuristic information obtained from Canny edge detection through ant colony algorithm. The gradient threshold *Th* of the Canny algorithm is employed to set a large range for the selection of edge points, and then a small range is eliminated by the number of pheromones at the end of the ant colony algorithm. Since the initial position of the ants in the ant colony algorithm is only limited to the possible edge area detected by Canny and can only walk in this area, a large number of irrelevant operations are avoided, and the operating efficiency of the ant colony algorithm is improved.

The navigation line information is further extracted. Normally, the navigation line of a mobile robot is vertical, so the frame of axes is set up. The origin of the frame of axes is in the lower left corner, and the x-axis is forward, horizontally to the right, and the y-axis is forward, vertically upward. The number of rows increases from 0 to n from near to far. The equation of the line with the left and right edges of the navigation line in the frame of axes is set as follows.

$$\begin{cases} y_1 = b_1 x + a_1 \\ y_2 = b_2 x + a_2 \end{cases} \tag{30}$$

The least squares method is adopted to fit the navigation line, and the equation is as follows.

$$\begin{cases} b = \dfrac{x_1 y_1 + \cdots + x_n y_n - n\overline{xy}}{x_1^2 + \cdots + x_n^2 - n\overline{x}^2} \\ a = \overline{y} - b\overline{x} \end{cases} \tag{31}$$

Among them, x and y are the abscissa and ordinate, respectively. The average value of the abscissa and ordinate are $\overline{x}, \overline{y}$, respectively. a, b are the linear coefficients after fitting. Therefore, to fit the edge of the navigation line, the left and right edge points are scanned first, which are then converted into world coordinates for conditional judgment. Appropriate points are retained to eliminate noise until the whole image is scanned, and then the fitting line coefficient is obtained by the least square method.

3.4. Simulations

To verify the performance of the model constructed in this research, an automatic navigation model of an intelligent mobile robot is built on the Matlab network simulation platform under hardware and software design to predict and analyze its performance. 2D laser sensors and machine vision are difficult to synchronize in time due to the difference in sampling frequency when performing obstacle distance and category combined detection experiments, which makes it impossible to achieve correlation matching between distance and category for the same obstacle detected. Therefore, this research adopts thread collection method to collect laser data and image information. The scanning range of the 2D laser sensor is set to $\pm 90^\circ$, and the preprocessing threshold is x_{max} =1. The constructed mobile robot navigation model adopts obstacle distance and category combination detection, and the experiment is selected to be carried out, which is divided into six work areas. In the simulation, the central processing unit (CPU) of the computer is CORE-i7–4720HQ-2.6 GHz. The neural network is built using Google's open source Tensorflow framework, which is a machine learning and deep learning programming framework under vector flow graphs. Matrix calculations are completed using Numpy and Pandas open-source toolkits. The Numpy library is an open-source matrix processing library. Pandas library provides good help for data cleaning and data preprocessing in data analysis.

In the analysis of the trajectory detection performance of mobile robots, the Canny-based ant colony algorithm proposed in this work is compared with the path optimization algorithms proposed by other scholars. Navigation path optimization algorithms include genetic algorithm (GA) [27], particle swarm optimization (PSO) [28], ant colony algorithm (ACA) [29], and particle swarm optimization and ant colony

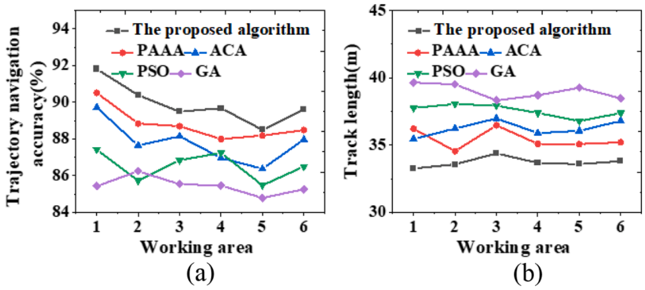

Fig. 8. Curves of trajectory navigation accuracy and path optimization length of different algorithms in each work area (a: trajectory navigation accuracy; b: path optimization length).

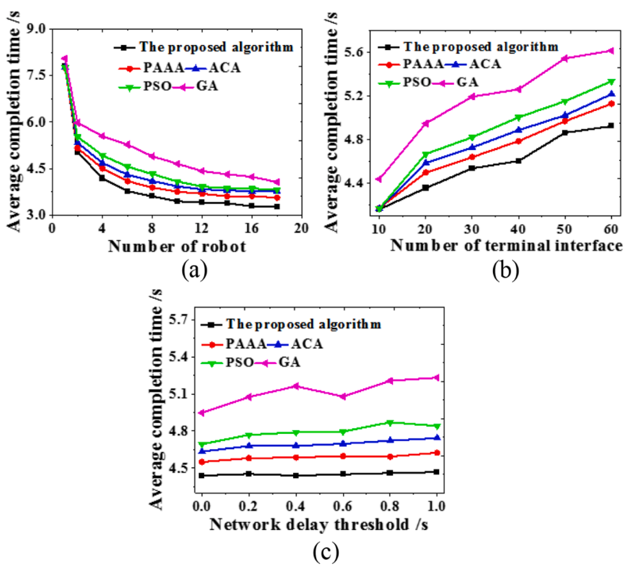

Fig. 9. Comparison of the influence of various algorithms on the average running time of navigation path detection under different factors (a: number of mobile robots; b: number of terminal interfaces; c: network delay threshold).

algorithm (PAAA) [30]. The analysis is carried out from the navigation accuracy [31] and data transmission performance of the mobile robot.

In terms of obstacle detection accuracy, the proposed SSD algorithm is compared with AlexNet [32], DenseNet [33], VGGNet [34], IGCNet [35], and ResNet [36] proposed by other scholars. The performance is analyzed from the perspective of accuracy, precision, recall, F1 value, and error. In order for the neural network framework to achieve the desired prediction results, the following hyperparameters are set. The number of training cycles (Epochs) is 30, the learning rate is 0.002, the batch size is 128, and the convolution kernel size is 1×3. The activation function is rectified linear unit (ReLU), the dropout rate in the convolutional neural network framework is 0.5, and the optimizer is Adam.

4. Results and discussion

4.1. Navigation trajectory performance of different algorithms

In the navigation path trajectory analysis of Canny-based ant colony algorithm built in this work, the algorithm is compared with GA, PSO, ACA, and PAAA. The navigation accuracy and path optimization length are shown in Fig. 8.

Fig. 8a shows that through the trajectory navigation accuracy analysis of each algorithm in different work areas, it is found that the Canny-based ant colony algorithm proposed in this work can significantly improve the trajectory navigation accuracy of the robot, which is

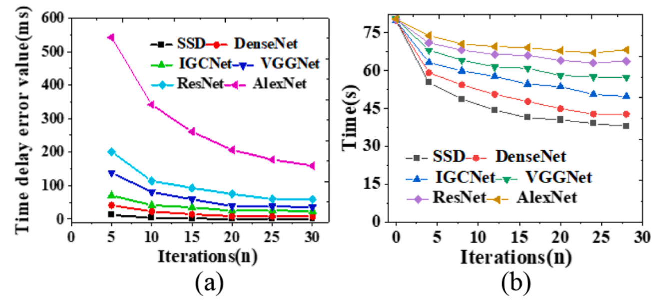

Fig. 10. Curves of delay and required time under different iteration times of different algorithms (a: delay; b: required time).

basically stable at around 89.62%. Fig. 8b shows the analysis of path optimization length. The path optimization length of the model algorithm proposed in this work is basically stable at about 33.81 m, while the path optimization length of the genetic algorithm is the longest. Therefore, the route navigation performance of this research algorithm is the best in the comparative analysis of navigation trajectories of different algorithms.

4.2. Data transmission performance of different algorithms

In terms of data transmission performance, the influence of the number of mobile robots, the number of terminal interfaces, and the change of the network delay threshold on the average running time is analyzed as shown in Fig. 9. Further analysis of the data transmission delay and required time under different iteration times of each algorithm is shown in Fig. 10.

Further analysis of the average running time of the navigation path detection of each algorithm indicates that with the increase of the number of mobile robots, the average running time of the navigation path detection of the model gradually decreases until it becomes stable, and the running time is basically stable at about 3.26 s (Fig. 9a). With the increase in the number of terminal interfaces, the average running time of navigation path detection shows an upward trend. However, compared with the model algorithm proposed by other scholars, it is obvious that Canny's ant colony algorithm proposed in this research requires less time (Fig. 9b). In addition, there is no significant change in multiple model algorithms as the network delay threshold increases. The

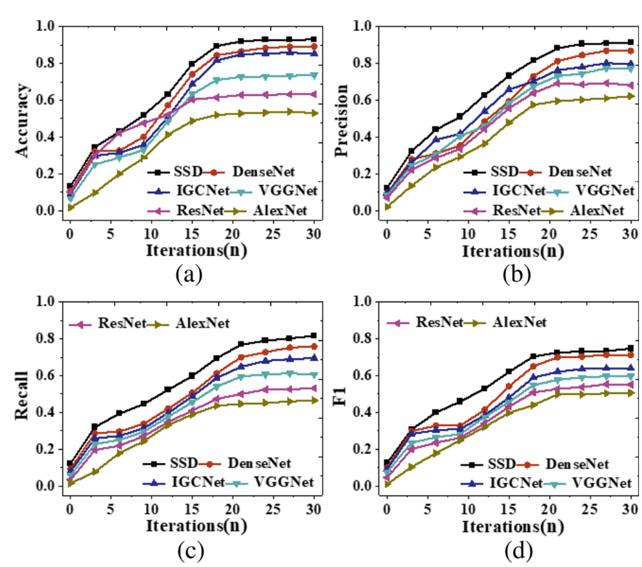

Fig. 11. The curve graph of the influence on the recognition accuracy with the increase of the number of iterations under different algorithms (a: accuracy; b: precision; c: recall; d: F1 value).

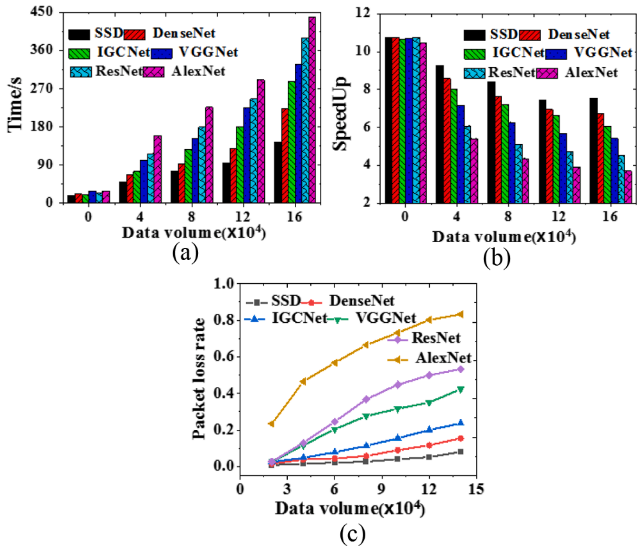

Fig. 12. Acceleration efficiency of different model algorithms under different data volumes (a: time required; b: speedup ratio; c: packet loss rate).

average running time of the algorithm in this research is stable at around 4.46 s, while the running time of GA shows an increasing trend (Fig. 9c). Therefore, it is verified through the analysis of the navigation path detection performance of each model algorithm, the proposed mobile robot automatic navigation model algorithm under Canny's ant colony algorithm is always better than other algorithms, and the average running time of navigation path detection is the smallest.

Fig. 10a shows that the error value gradually decreases as the number of iterations increases. The delay time of AlexNet algorithm is the largest, which is 542.15 ms, while the delay time of the proposed algorithm approaches 0. The analysis results of the time required for each algorithm are shown in Fig. 10b. As the number of iterations increases, the time required for the mobile robot's automatic navigation model to detect obstacles decreases and gradually tends to remain unchanged, and finally basically stabilizes at 37.99 s. Therefore, the proposed obstacle detection time delay under the SSD algorithm is relatively lower, and the required time is shorter.

4.3. Recognition accuracy of each neural network algorithm

The model constructed in this work is compared with the advanced CNN, and the recognition performance of the detection model is analyzed regarding accuracy, precision, recall, and F1 values, as illustrated in Fig. 11.

In Fig. 11, the model in this work is compared with other neural network algorithms in terms of accuracy, precision, recall, and F1. The recognition accuracy of the proposed algorithm reaches 92.90%, which is at least 3.74% higher than the model algorithm proposed by other scholars. Further comparisons of precision, recall, and F1 show that the precision, recall, and F1 of the model algorithm in this work are 91.11%, 81.57%, and 74.70%, respectively. Compared with other algorithms, the precision, recall, and F1 values of the model algorithm in this work are obviously higher, at least 3.29% higher than other algorithms. Compared with the model algorithms proposed by other scholars in related fields, the SSD model algorithm constructed in our research has better accuracy in obstacle detection, identification, and prediction.

4.4. Comparison of acceleration efficiency of various neural network algorithms

The constructed mobile robot automatic navigation model algorithm is compared with AlexNet, DenseNet, VGGNet, IGCNet, and ResNet model algorithms utilized by other scholars in related fields, and the required time, acceleration ratio, and packet loss rate are analyzed from different data volumes. The results are shown in Fig. 12.

The analysis results of the acceleration efficiency of each algorithm are shown in Fig. 12. Compared with the model algorithms utilized by other scholars, the improved SSD neural network algorithm is less sensitive to data growth in mobile robot operation scenarios and more suitable for processing large amounts of data. Moreover, the acceleration effect is more pronounced, the acceleration ratio is higher. The packet loss rate refers to the ratio of the number of packets lost in data transmission to the data group sent. However, with the increase of data amount, the data packet loss rate of the model algorithm proposed in this work does not increase significantly and basically stays below 0.1. Therefore, in the comparative analysis of experimental results of all methods, the automatic navigation model of mobile robot under machine vision proposed in this work is still able to achieve favorable navigation path effect, and the data transmission performance is good.

5. Conclusion

Today, with the rapid progression of science, the intelligence of all walks of life is accelerating, and the adoption of robots is becoming more and more widespread. In this work, the ant colony algorithm under Canny is proposed to detect the edge of the trajectory, aiming at the shortcomings of the current robot such as poor working flexibility. SSD algorithm is employed to detect obstacles in the robot navigation path. Through simulation and performance analysis, it is found that the navigation accuracy is basically stable at 89.62%, the running time is stable at about 37.99 s, and the packet loss rate is close to 0. It can provide experimental reference for the wide adoption and intelligent progression of robots in all walks of life. However, this work also has some deficiencies. For example, the image processing strategy in this work is under less interference and clear navigation line edge in the collected images. Although the efficiency of the image processing algorithm is high, the navigation line may be lost when the illumination condition is poor and there are too many interferers. Therefore, it is necessary to further study the image processing algorithm to improve the environment adaptability of the mobile robot model, which is of great significance to the intelligent progression of the robot field.Eq. (1), 2, 3, 4, 5, 6, 7, 8, 9, 10, 11, 12, 13, 14, 15, 16, 18, 19, 20, 21, 22, 23, 26, 27, 29, 30, (31)

Declaration of Competing Interest

None

Acknowledgement

This work was supported by Chongqing Big Data Engineering Laboratory for Children, Chongqing Electronics Engineering Technology Research Center for Interactive Learning, Chongqing University Innovation Research Group, Project of Science and Technology Research Program of Chongqing Education Commission of China.(N0. KJZD-K201801601) (Pengcheng Wei). This work was supported by Dr Di Zhenpeng Science Research Startup King (K9–9999–15–00–00–015), Funding for the Construction of Management Science and Engineering discipline of Guangxi institute of Finance and Economics, Guangxi higher Education undergraduate Teaching Reform Project 2020 (2020JGZ147), Planning Fund Project of Ministry of education (20YJA790039).(ZhenPeng Di)

References

[1] K. Inoue, Y. Kaizu, S. Igarashi, K. Imou, The development of autonomous navigation and obstacle avoidance for a robotic mower using machine vision technique, IFAC-PapersOnLine 52 (30) (2019) 173–177.

[2] E. Mavridou, E. Vrochidou, G.A. Papakostas, T. Pachidis, V.G. Kaburlasos, Machine vision systems in precision agriculture for crop farming, J. Imaging 5 (12) (2019) 89.
[3] S.G. Tzafestas, Mobile robot control and navigation: a global overview, J. Intelligent & Robotic Syst. 91 (1) (2018) 35–58.
[4] Y. Wu, X. Ta, R. Xiao, Y. Wei, D. An, D. Li, Survey of underwater robot positioning navigation, Appl. Ocean Res. 90 (2019), 101845.
[5] A.M. Abdulazeez, F.S. Faizi, Vision-Based mobile robot controllers: a scientific review, Turkish J. Comput. Math. Educ. (TURCOMAT) 12 (6) (2021) 1563–1580.
[6] Y.D. Yasuda, L.E.G. Martins, F.A. Cappabianco, Autonomous visual navigation for mobile robots: a systematic literature review, ACM Comp. Surveys (CSUR) 53 (1) (2020) 1–34.
[7] C. Zhang, L. Yong, Y. Chen, S. Zhang, L. Ge, S. Wang, W. Li, A rubber-tapping robot forest navigation and information collection system based on 2D LiDAR and a gyroscope, Sensors 19 (9) (2019) 2136.
[8] S. Wang, S. Zhang, R. Ma, E. Jin, X. Liu, H. Tian, R. Yang, Remote control system based on the Internet and machine vision for tracked vehicles, J. Mech. Sci. Technol. 32 (3) (2018) 1317–1331.
[9] L. Cheng, B. Song, Y. Dai, H. Wu, Y. Chen, Mobile robot indoor dual Kalman filter localisation based on inertial measurement and stereo vision, CAAI Trans. Intelligence Technol. 2 (4) (2019) 173–181.
[10] F. Bayat, S. Najafinia, M. Aliyari, Mobile robots path planning: electrostatic potential field approach, Expert Syst. Appl. 100 (2018) 68–78.
[11] S. Hosseininejad, C. Dadkhah, Mobile robot path planning in dynamic environment based on cuckoo optimization algorithm, Int. J. Adv. Robotic Syst. 16 (2) (2019), 1729881419839575.
[12] Q. Wu, Z. Chen, L. Wang, H. Lin, Z. Jiang, S. Li, D. Chen, Real-time dynamic path planning of mobile robots: a novel hybrid heuristic optimization algorithm, Sensors 20 (1) (2020) 188.
[13] D. Wang, S. Chen, Y. Zhang, L. Liu, Path planning of mobile robot in dynamic environment: fuzzy artificial potential field and extensible neural network, Artificial Life and Robotics 26 (1) (2021) 129–139.
[14] X.I.E. Xin, X.I.A. Zhelei, Image recognition of cervical cancer cells based on deep convolution neural networks, J. China Univ. Metrol. 2 (2018) 14.
[15] N. He, M.E. Paoletti, J.M. Haut, L. Fang, S. Li, A. Plaza, J. Plaza, Feature extraction with multiscale covariance maps for hyperspectral image classification, IEEE Trans. Geosci. Remote Sensing 57 (2) (2018) 755–769.
[16] O. Sergiyenko, V. Tyrsa, 3D optical machine vision sensors with intelligent data management for robotic swarm navigation improvement, IEEE Sens. J. 21 (10) (2020) 11262–11274.
[17] G.T. Papadopoulos, M. Antona, C. Stephanidis, Towards open and expandable cognitive AI architectures for large-scale multi-agent human-robot collaborative learning, IEEE Access 9 (2021) 73890–73909.
[18] E. Mattar, K. Al Mutib, M. Al Sulaiman, H. Ramdane, Mobile robot intelligence based SLAM features learning and navigation, Int. J. Comp. Digital Syst. 7 (01) (2018) 23–34.
[19] S. Bonadies, S.A. Gadsden, An overview of autonomous crop row navigation strategies for unmanned ground vehicles, Eng. Agriculture, Environ. Food 12 (1) (2019) 24–31.
[20] M.H.F.M. Fauadi, S. Akmal, M.M. Ali, N.I. Anuar, S. Ramlan, A.Z.M. Noor, N. Awang, Intelligent vision-based navigation system for mobile robot: a technological review, Periodicals of Eng. Nat. Sci. 6 (2) (2018) 47–57.
[21] L. Wang, L. Zhao, G. Huo, R. Li, Z. Hou, P. Luo, C. Yang, Visual semantic navigation based on deep learning for indoor mobile robots, Complexity, 2018 (2018).
[22] B. Li, J.P. Muñoz, X. Rong, Q. Chen, J. Xiao, Y. Tian, M. Yousuf, Vision-based mobile indoor assistive navigation aid for blind people, IEEE Trans. Mobile Comp. 18 (3) (2018) 702–714.
[23] S. Karakaya, G. Kucukyildiz, H. Ocak, A new mobile robot toolbox for MATLAB, J. Intelligent & Robotic Syst. 87 (1) (2017) 125–140.
[24] S.H. Kim, S.J. Lee, S.W. Kim, Weaving laser vision system for navigation of mobile robots in pipeline structures, IEEE Sens. J. 18 (6) (2018) 2585–2591.
[25] Y.C. Tang, C. Wang, L. Luo, X. Zou, Recognition and localization methods for vision-based fruit picking robots: a review, Front. Plant Sci. 11 (2020) 510.
[26] X. Gao, J. Li, L. Fan, Q. Zhou, K. Yin, J. Wang, Z. Wang, Review of wheeled mobile robots' navigation problems and application prospects in agriculture, IEEE Access 6 (2018) 49248–49268.
[27] P. Huang, Z. Zhang, X. Luo, J. Zhang, P. Huang, Path tracking control of a differential-drive tracked robot based on look-ahead distance, IFAC-PapersOnLine 51 (17) (2018) 112–117.
[28] P.K. Das, P.K. Jena, Multi-robot path planning using improved particle swarm optimization algorithm through novel evolutionary operators, Appl. Soft Comput. 92 (2020), 106312.
[29] A. Vysocký, R. Papřok, J. Šafařík, T. Kot, Z. Bobovský, P. Novák, V. Snášel, Reduction in robotic arm energy consumption by particle swarm optimization, Appl. Sci. 10 (22) (2020) 8241.
[30] C. Wei, Z. Ji, B. Cai, Particle swarm optimization for cooperative multi-robot task allocation: a multi-objective approach, IEEE Robotics and Automation Lett. 5 (2) (2020) 2530–2537.
[31] G. Yang, Z. Chen, Y. Li, Z. Su, Rapid relocation method for mobile robot based on improved ORB-SLAM2 algorithm, Remote Sens. (Basel) 11 (2) (2019) 149.
[32] Y. Wang, J. Yang, M. Liu, G. Gui, LightAMC: lightweight automatic modulation classification via deep learning and compressive sensing, IEEE Trans. Vehicular Technol. 69 (3) (2020) 3491–3495.
[33] Y. Wang, Q. Chen, D. Gan, J. Yang, D.S. Kirschen, C. Kang, Deep learning-based socio-demographic information identification from smart meter data, IEEE Trans. Smart Grid 10 (3) (2018) 2593–2602.
[34] D. Zhang, M.R. Kabuka, Combining weather condition data to predict traffic flow: a GRU-based deep learning approach[J], IET Intelligent Transp. Syst. 12 (7) (2018) 578–585.
[35] Y. Xing, C. Lv, H. Wang, D. Cao, E. Velenis, F.Y. Wang, Driver activity recognition for intelligent vehicles: a deep learning approach, IEEE Trans. Vehicular Technol. 68 (6) (2019) 5379–5390.
[36] S. Deepak, P.M. Ameer, Brain tumor classification using deep CNN features via transfer learning, Comput. Biol. Med. 111 (2019), 103345.

Pengcheng Wei was born in Hechi, Guangxi, P. R. China in 1975. Wei earned his Ph.D in Engineering in 2008. Now he is the professor at Chongqing University of Education known for his work on computational intelligence, information security and big data analysis.E-mail: gxwpc@cque.edu.cn.

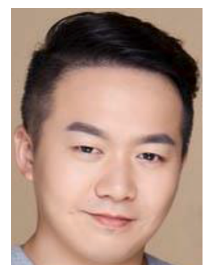

Xianping Yu was born in Beijing, P. R. China, in 1983. He received the master degree in Software engineering from Beijing University of Posts and Telecommunications, Beijing, China, in 2010. He is now working at Commuicaton and Art Experimental Teaching Center from Beijing Normal University as a teacher. His-research interest include computational intelligence, information security and big data analysis.E-mail: 05,079@bnu.edu.cn.

Zhenpeng Di was born in Dongtai, Jiangsu. P.R. China, 1967. He received a doctorate from the University of Science and Technology of Macau. Now a researcher at Guangxi University of Finance and Economics, his research direction is enterprise management and innovation management.E-Mail: 2,018,110,034@gxufe.edu.cn.

Xiaojun Dai was born in Huanggang, Hubei. China in 1995. Master student. Graduate student of Chongqing University of Posts and Telecommunications. His-research interests is facial expression recognition, Artificial Intelligence.E-mail: s200331057@stu.cqupt.edu.cn.

Bo Wang was born in Chongqing, P.R. China in 1997.Master student. Wang is study in Chongqing University of Posts And Telecommunications. Wang specialism is Computer vision, Artificial Intelligence.E-mail: wb2690495903@163.com.

Yushan Zeng was born in Zigong, Sichuan, China in 1998, Master student. Graduate student of Chongqing University of Posts and Telecommunications. His-research interests are Artificial Intelligence and deep learning.E-mail: ZYS15983150882@163.com.